Epileptic Disord 2016; 18 (4): 418-25

Propagation of seizures in a case of lesional mid-cingulate gyrus epilepsy studied by stereo-EEG*

Rafeed Alkawadri [1], Jorge Gonzalez-Martinez [2], Nicolas Gaspard [1,3], Andreas V. Alexopoulos [2]

[1] The Department of Neurology, School of Medicine, Yale University New Haven, CT
[2] The Epilepsy Center at Cleveland Clinic Foundation. Cleveland, Ohio, USA
[3] Hôpital Erasme, ULB Cliniques universitaires de Bruxelles, Bruxelles, Belgium

Received December 14, 2015; Accepted October 2, 2016

ABSTRACT – Little is known about the propagation of seizures arising from the cingulate gyrus, as cingulate coverage with interhemispheric subdural electrodes is usually challenging and incomplete due to inherent anatomical and vascular limitations. We present a case of lesional mid-cingulate epilepsy confirmed by stereotactically implanted intracranial depth electrodes and subsequent surgical resection. Hypermotor symptomatology was seen during the first seven seconds of seizure onset while the seizure was still confined to the mid-cingulate gyrus contacts. The patient had brief contralateral clonic movements as seizure propagated to the primary motor cortex. There was a high concordance between the primary propagation contacts, as delineated by intracranial EEG, and the contacts, with higher coherence values in the connectivity matrix. Interestingly, cingulate-extra-cingulate connectivity and spread to the primary motor, premotor, and prefrontal cortex was seen preceding spread to other cingulate contacts, of which one was less than 15 mm from the onset contact. This report is one of a few published, documenting propagation of seizures arising from the mid-cingulate cortex. As illustrated by these data, hypermotor semiology correlated with direct activation of the cingulate cortex. Subsequent seizure propagation activated an extensive extra-cingulate rather than an intra-cingulate epileptogenic network. Interestingly, had the region of onset not sampled, the seizure onset would have appeared as non-localizing widespread rhythms over the fronto-parietal convexities. Further studies to explore the propagation of seizures arising from the cingulate gyrus and the physiological and pathological connectivity patterns within the cingulate gyrus in humans are needed, preferably using stereotactic implantation. Specific targets to be investigated are also discussed.

Key words: cingulate epilepsy, SEEG, hypermotor seizures, connectivity, propagation

Correspondence:
Rafeed Alkawadri
15 York Street, LCI 7-14B,
New Haven, CT 06520, USA
<mhdrafeed.alkawadri@yale.edu>

*This work was presented in a poster session at the annual meeting of the American Clinical Neurophysiology Society, Miami Florida, 2013.

doi:10.1684/epd.2016.0874

Literature on the propagation of seizures arising from the cingulate gyrus is limited (Koubeissi *et al.,* 2009, Alkawadri *et al*., 2011, 2013), as cingulate coverage with interhemispheric subdural electrodes is challenging and usually incomplete due to inherent anatomical and vascular limitations. These challenges can be partially overcome by stereotactically implanted depth electrodes, which allow for better sampling from deep-seated and mesial structures. Mazars published *"Criteria for identifying cingulate epilepsies"* and reported 36 cases. This study predated magnetic resonance imaging (MRI) and computed tomography (CT), and localization by intra-cerebral depth electrodes was problematic by today's standards (Yakovlev and Locke, 1961; Mazars, 1970; Arikuni *et al*., 1994; Seltzer and Pandya, 2009).

Bancaud and Talairach (1992) published a review of patients with anterior cingulate epilepsy. The review summarized the findings of 66 seizures in 16 patients. In this article, cases were not discussed individually. The knowledge about connectivity of the cingulate gyrus is based on studies in rhesus monkeys and observations in the postmortem human brain (Garzon and Lüders, 2008). Herein, we present a case of mid-cingulate gyrus epilepsy confirmed by stereotactically implanted depth electrodes and by subsequent surgical resection. We discuss the propagation patterns and connectivity of the seizure onset zone using magnitude squared coherence. We also discuss the clinical semiology in relation to ictal rhythms.

Methods

A patient with lesional anterior cingulate epilepsy underwent intracranial invasive evaluation using stereotactically implanted depth electrodes at the Cleveland Clinic Epilepsy Center. Twelve electrodes containing 130 contacts were implanted over the left hemisphere covering areas in the left frontal and parietal regions (*see figure 1 for location of electrodes co-registered with pre-operative T1 MRI*). Clinical, invasive, and non-invasive data were reviewed and summarized (*figure 1A, B*). Invasive EEG recording was performed using the Nihon-Kohden system (Tokyo, Japan) at 500-Hz sampling rate.

Coherence analysis

Ten-minute resting awake EEG data was divided into 500-millisecond windows with 50-millisecond overlap between adjacent windows. A hamming window was then used with the same length and spectrogram was generated for each window using Fast Fourier Transform (FFT). A connectivity matrix was computed using the spectral coherence between seizure onset contacts (X'1, X'2) in the mid-cingulate cortex and other grey matter contacts. The grey matter contacts were identified from 3D co-registration of post-implantation CT of the head with pre-implantation MRI of the brain (*figure 1C*). Coherence estimates of the seizure onset region were then calculated for 45 seconds (100 windows) and averaged over 13 trials (Zaveri *et al.,* 1999),

$$C_{ij} = \frac{\left|Px_i x_j\right|^2}{Px_i x_i - Px_j x_j}$$

where P_{XiXi} is the cross spectrum and P_{XiXi} and P_{XjXj} respectively correspond to the power spectra of signals X_i and X_j at a given frequency. The mean coherence was calculated for a band between 3 and 50 Hz at each window. Each onset contact (X'1, and X'2) rendered an array of coherence values, and then the mean of two arrays was used to represent final coherence values of seizure onset contacts. Non-parametric statistical methods were used for comparisons of coherence values between electrodes.

Seizure analysis

Three spontaneous seizures (*i.e.* seizures not triggered by electrical stimulation) were recorded and each seizure was inspected visually to determine a baseline interictal period and the time of onset of the EEG seizure, *i.e.* the exact timing of the first relevant electrical changes that occurred prior to clinical onset of the seizure. The seizure onset zone was defined from stereo-EEG recordings using standard visual analysis by an expert reader. In order to standardize detection and interpretation of EEG involving each contact, we modified and applied a statistical method of EEG analysis, as proposed by David and colleagues (David *et al.,* 2011). Similar analysis can also be found by Wendling and colleagues (Wendling *et al.,* 2003). Seizures were similar in their clinical behaviours and early EEG patterns. Secondary generalization was seen in Seizure 3, which is presented in the results. Baseline recordings were chosen as 20-second segments in the period preceding the seizure. Areas with significant artefact were not included in this analysis.

The stereo-EEG signal of each electrode was transformed in time and frequency ranges using Fast Fourier Transformation (temporal resolution *dt* of 100 m; spectral resolution *df* of 1 Hz; and range: 1-50 Hz). To capture temporal changes of the power in a certain frequency range, overlapping epochs of data were successively selected from the time-frequency plane. The duration of epochs can be adapted to the expected duration of bursts of stereo-EEG oscillations. In this study, we used D=1 sec. Unpaired t-test was then used to evaluate for significant changes in power compared to baseline. We accepted alpha-error margin at 0.05, family-wise corrected for multiple comparisons.

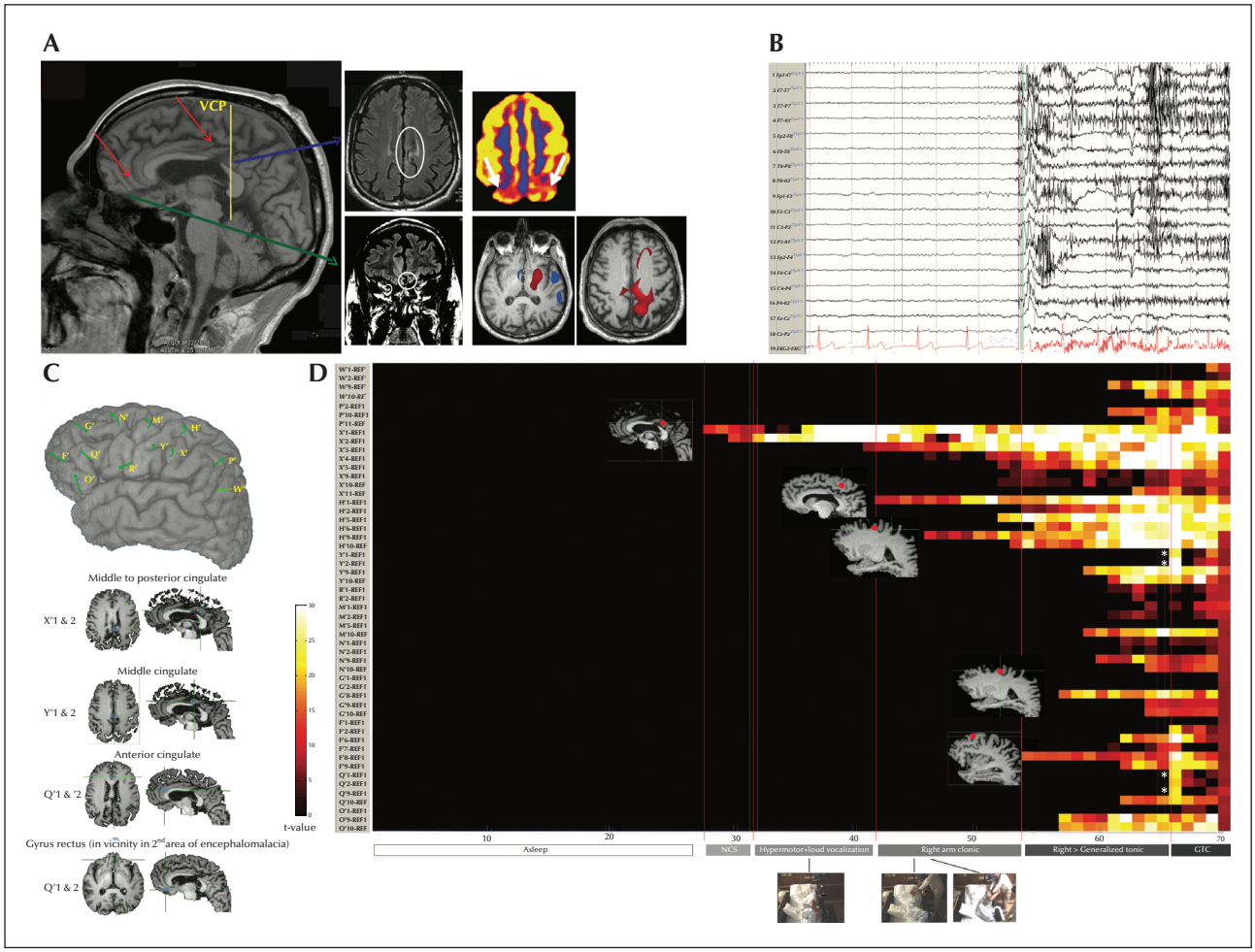

Figure 1. Summary of presurgical workup, intracranial stereo-EEG implantation, and statistical analysis of transformed EEG data during a seizure recorded by depth electrodes. (A) Summary of neuroimaging findings. Sagittal T1-weighted MRI showing the mid-cingulate and anterior cingulate abnormalities on the left side (red arrows), and the relationship of the mid-cingulate lesion to the VPC line (yellow), *i.e.* the vertical line through the posterior commissure. Encircled on the axial and sagittal FLAIR images are areas of increased signal intensity surrounding the lesion within the mid-cingulate gyrus (blue arrow), and the encephalomalacia within the orbitofrontal region (green arrow) respectively. The upper right-sided image depicts a colour-coded FDG-PET scan showing hypometabolism in the bilateral fronto-parietal regions, more pronounced on the left. The lower two axial images are the results of SISCOM analysis of the patient's ictal SPECT study which showed two discrete areas of hyperperfusion in proximity to the two MRI lesions, with the predominant focus originating from the mid-cingulate lesion. (B) Ten-second window of scalp EEG data at seizure onset viewed in anterior posterior bipolar montage. Notice the widespread electric decrements along with low-amplitude evolving alpha/theta rhythms. The patient had 2 stereotypical habitual events recorded during this scalp video-EEG evaluation. Clinically, the seizures consisted of brief hypermotor behaviour, while EEG rhythms were obscured by movement artefacts. (C) Stereo-EEG coverage of the left hemisphere. Individual axial and sagittal images show the location of electrode contacts that were implanted within the cingulate and orbitofrontal regions. (D) Statistically-transformed EEG data of Seizure 3 weighted by t-value compared to baseline. The horizontal axis represents time and the vertical axis individual electrode contacts. The corresponding sagittal MRI images show location of electrodes involved sequentially by the ictal discharge. The asterisks mark other anterior cingulate contacts, which are relatively uninvolved until late during the course of the seizure. The grey-scaled boxes at the bottom denote the clinical behaviour observed during the seizure, and the duration of each component corresponds to the width of the box.
FLAIR: fluid attenuated inversion recovery; FDG-PET: fluoro-deoxy-glucose positron emission tomography; SPECT: single photon emission computed tomography; SISCOM: subtracted ictal SPECT co-registered with MRI; NCS: no clinical signs (*i.e.* subclinical electrographic seizure); GTC: generalized tonic-clonic seizure.

Significant changes from baseline were required to be present in four consecutive epochs (*i.e.* for a period of four seconds) before they were accepted as being part of the evolving ictal rhythm. Statistics of power at seizure onset were obtained for every frequency and for a band spanning the 14-25-Hz range. We chose this band because it is suitable for analysis of low-voltage fast activity and repetitive spiking. Indeed, beta frequency was the dominant evolving frequency in this case and is the most common ictal pattern

described in both neocortical and temporal lobe seizures (Schiller *et al.*, 1998; Lee *et al*., 2000; Velasco *et al.*, 2000). The same frequency-specific averaging is performed on baseline data with the same time resolution of *dt* 100 ms between successive epochs.

Case study

The patient was a 48-year-old right-handed man with a history of seizures for the past 20 years, with onset one year after closed head trauma. Habitual seizures typically started with an aura described as "unusual scary and weird feeling" which could last for several minutes and was typically followed by a motor seizure, especially when drowsy. The typical seizure was characterized by sitting up in bed, turning to the left, and attempting to get down on the floor, followed by kicking and thrashing without loss of consciousness. Seizures rarely generalized. He continued to have one seizure a week and has failed trials of several antiepileptic medications. His neurological examination was unremarkable.

Interictal scalp video-EEG evaluation was repeatedly unremarkable with normal background, symmetric sleep structures, and absence of epileptiform discharges. Movements and muscle artefacts obscured ictal EEG activities. However, a pattern of diffuse background suppression followed by non-lateralized evolving theta rhythms (most prominent in the parasagittal chains) could be appreciated on careful inspection. MRI of the brain showed mild generalized parenchymal volume loss and abnormal T2/FLAIR signal in the posterior body of the corpus callosum, adjacent to the left mid-cingulate cortex. In addition, an area of subtle encephalomalacia was identified in the orbitofrontal region involving the gyrus rectus on the left side.Interictal FDG-PET showed symmetrically decreased metabolism in the bilateral dorsolateral parietal regions. A subtraction ictal SPECT co-registered with MRI (SISCOM) analysis of ictal and interictal SPECT showed two areas of hyperperfusion in proximity to the MRI lesions with the predominant focus originating from the mid-cingulate lesion. Neuropsychological testing was suggestive of mild frontal dysfunction. The patient was referred for an invasive evaluation with stereo-EEG electrodes following discussion in our multidisciplinary surgical patient management conference.

The stereo-EEG exploration focused on the mesial aspects of the left hemisphere, in particular the cingulate gyrus and orbitofrontal and parietal regions to determine the site of seizure onset (*figure 2*). Interictally, rare spikes were seen arising from the posterior edge of the cingulate lesion. Three seizures were recorded with stereo-EEG electrodes. All seizures originated from the vicinity of the cingulate lesion and had identical semiology and early propagation EEG patterns. We present the data of the third seizure as a representative of the recorded seizures. Notably, the hypermotor symptomatology, seen early during the course of the clinical seizure, occurred while the electrographic discharge was still confined to the mid-cingulate contacts. A right arm clonic seizure ensued as discharges spread to involve the primary motor cortex, followed by a brief contralateral tonic/dystonic posturing with further spread to the pre-frontal cortex. In addition to this evolving ictal activity in the beta range, we observed a non-evolving widespread "buzz" of paroxysmal fast activity (25-40 Hz) within three seconds of onset, lasting for a period of 3-10 seconds (*figure 3A*). Finally, coherence values between onset contacts and early propagation contacts and contacts with paroxysmal fast activity were statistically higher than the corresponding values of anterior cingulate contacts and other "control" contacts (*figure 3B*). Resection included the seizure onset zone and surrounding cingulate cortex. Pathology showed focal cortical dysplasia type IIB (*i.e.* with Balloon cells). The patient remained free of motor seizures in the six-month follow-up period after surgery. He has recovered from a mild contralateral sensory impairment.

Discussion

Lesional cingulate gyrus epilepsy is rare (Alkawadri *et al.*, 2011, 2013; Unnwongse *et al*., 2012). We present a case of lesional mid-cingulate gyrus epilepsy confirmed by stereotactically implanted intracranial depth electrodes and discuss the propagation pattern along with connectivity measures.

Ictal hypermotor behaviour was seen within four seconds of EEG seizure onset, while the ictal discharge remained confined to the mid-cingulate region. The patient had brief contralateral clonic movements, followed by tonic posturing as seizures propagated to nodes of the epileptogenic network outside the cingulate gyrus, namely to the primary motor and premotor areas, respectively. Talairach and colleagues demonstrated that stimulation of the anterior cingulate cortex leads to motor responses that are "different from those elicited by stimulation of the motor area" (Talairach *et al.*, 1973). Our findings are also consistent with Bancaud's report of behavioural changes in relation to electrical stimulation of the anterior cingulate gyrus (Bancaud *et al.*, 1976).

Use of Brodmann's maps led to wide and long-lasting acceptance of the simplistic (*i.e.* anterior and posterior) divisions of the cingulate gyrus (Brodmann, 1909). Vogt has demonstrated that the cingulate gyrus consists of four major divisions from a structural and

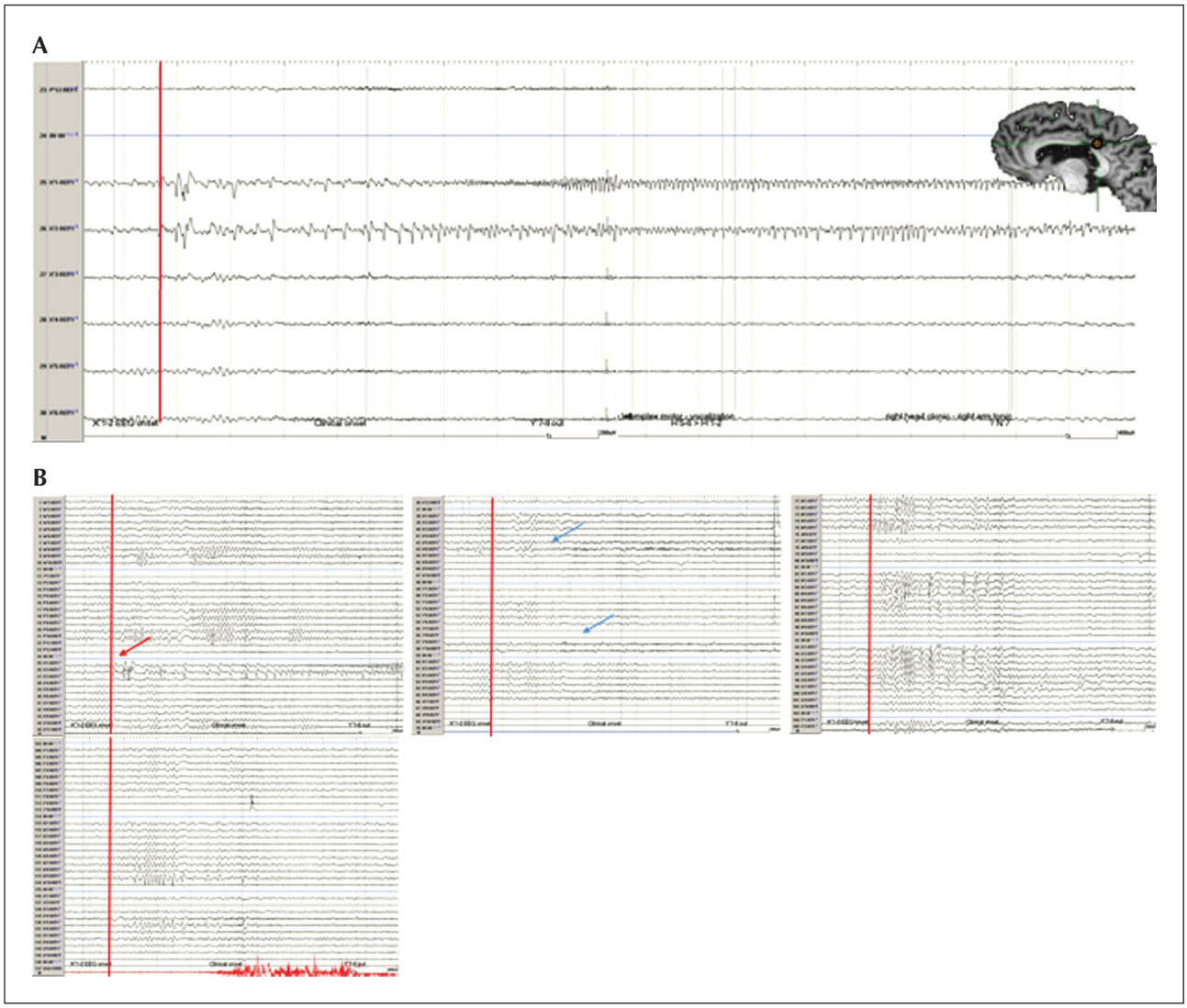

Figure 2. Intracranial EEG tracing of seizures using LF 3-Hz, and HF 100-Hz filter settings and referential montage (reference in diploic space). (A) Zoom in on the contact of onset. (B) EEG background in all contacts at the time of onset marked in red, and by the red arrow pointing at contacts of onset X1, X2. The blue arrows mark contacts with earliest spread of paroxysmal fast activity outside the cingulate. Each vertical line marks a second. Notice the burst of non-evolving theta at onset in frontal contacts.

functional standpoint (Vogt *et al*., 1992, 2001, 2005, 2006; Devinsky *et al*., 1995; Vogt and Laureys, 2005). These regions can be further subdivided into several functionally and cytoarchitecturally distinct components. With this in mind, it is not surprising that early propagation to the primary and accessory motor areas was observed prior to spreading to other cingulate regions. Widespread electro-decrement seen at seizure onset on scalp EEG correlated with widespread increase of frontal beta and gamma power on intracranial EEG recordings. Coherence values of the electrode contacts that were involved in the early paroxysmal fast burst and early seizure propagation were higher compared to the values obtained from other uninvolved anterior cingulate contacts.

Interestingly, in this case, had the region of onset not sampled, the seizure onset would appear as non-localizing widespread rhythms over the fronto-parietal convexities and less so within other cingulate subregions. In fact, and although, the implantation in this lesional case was influenced by the anatomic localization of the lesions, and the intimately connected regions, some experts may argue that the sampling from the cingulate is inadequate, and that cingulate sampling should include additional areas such as the posterior cingulate (areas 30, and 31) and subcallosal region (area 25). No electrical stimulation was performed for the purpose of seizure induction, we believe recording of a localized seizure onset and seizure freedom following a limited resection is the

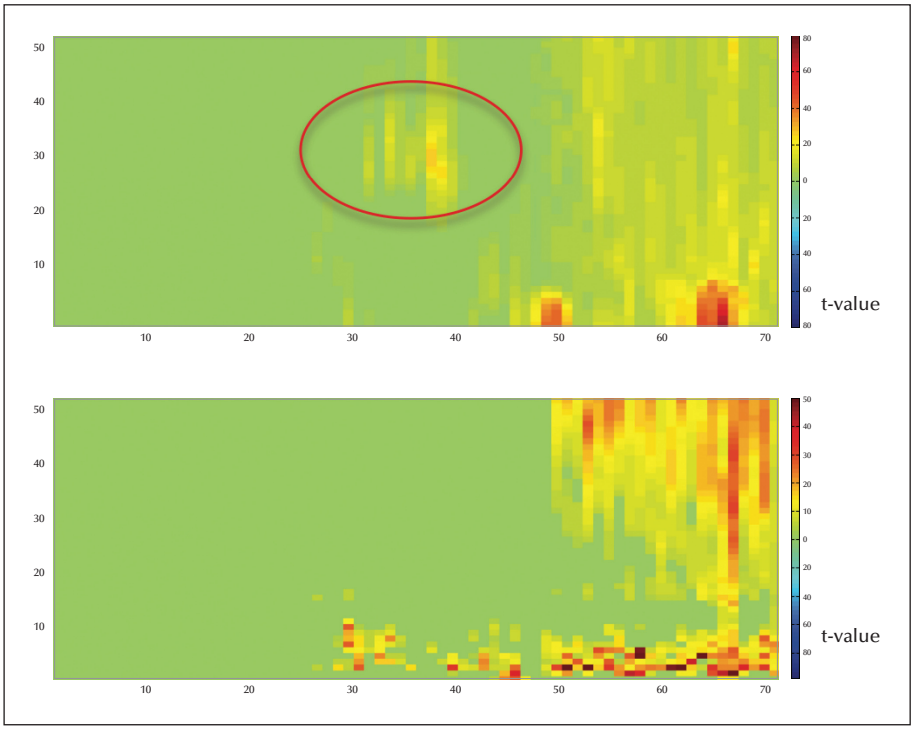

Figure 3. Statistical transformation in time-frequency space of EEG activity recorded by two electrode contacts weighted by t-value for significant changes compared to baseline. The upper plot is an example of an electrode contact recording an early non-evolving buzz of paroxysmal fast activity. The lower one depicts an electrode contact that does not record any paroxysmal fast changes early during the course of the seizure.

most suggestive feature that the epileptogenic zone was correctly regionalized.

This case report suggests that the symptomatology of hypermotor behaviour is associated with restricted ictal activation of the cingulate gyrus in the absence of extracingulate spread. With that said, the role of subcortical structures in the generation of hypermotor symptomatology cannot be entirely excluded (Guedj *et al.*, 2012; Wong *et al.*, 2010). Better understanding of the role of subcortical structures in defining seizure networks and their semiological expression thus offers an intriguing direction for future research. Furthermore, this report provides additional electrophysiological evidence to support the heterogeneity of the cingulate cortex, which is in line with the known features of cytoarchitecture and connectivity of the cingulate gyrus.

Any conclusions regarding clinical manifestations of mid-cingulate seizures must include sampling from the frontal and adjacent parietal regions in order to determine the relationship between clinical manifestations and the patterns of seizure propagation.

Interestingly, electrodes involved early following the seizure onset spanned a large spatial area and were located primarily outside the cingulate (as opposed to other contacts within the cingulate).

Based on the findings of our study and results of previous functional and histological studies of the cingulate, when cingulate epilepsy is suspected based on electroclinical basis, an invasive exploration with electrodes targeting at least four sub-regions of the cingulate is recommended: anterior cingulate cortex (ACC)-areas 32 and 25, anterior mid-cingulate cortex (aMCC)- area a24, posterior mid-cingulate cortex (pMCC)-areas p24 and 23d, and posterior cingulate cortex (PCC)-areas 23b, 30 and 31. In our case, the seizure onset zone might have been mislocalized to the lateral frontal region, had the mid-cingulate contact been placed a few centimetres away from its actual location (compare X'1 vs. Y'1 rhythms; *figure 1D*), despite the apparent proximity (14 mm) of the respective contacts in 3D space.

Cingulate coverage with interhemispheric subdural electrodes is usually challenging and incomplete, due to inherent anatomical and vascular limitations. Stereotactically implanted depth electrodes are technically superior in tackling deeply seated structures. We believe that the characteristic pathological EEG signature of focal cortical dysplasia was not seen because the epileptic region was restricted/confined, X contacts were in the immediate vicinity of seizure onset (*i.e.* likely not sampling from directly within

the lesion), and the epileptogenic region was relatively small. Although this is the first study reporting on propagation of seizures originating from the mid-cingulate gyrus using stereo-EEG, no generalization may be drawn from this single case report. It is possible that different propagation patterns exist and are influenced by the underlying pathology and localization of the epileptogenic lesion. It is also possible that the connectivity patterns reported herein do not match those seen in healthy or "non-epileptogenic" cingulate and other motor areas. This study highlights the need for future work exploring functional, electrophysiological, and anatomical connectivity of the cingulate cortex in humans. It is worthwhile emphasizing that currently, to our knowledge, there is no available reliable biomarker of epileptogenicity to identify epileptogenic tissue. In this study, we used good surgical outcomes following resection as a surrogate gold standard of the epileptogenic zone and the localization of epilepsy. Although this approach is commonly used in surgical series, we acknowledge that the concept of viewing a complex epileptogenic process, as a solitary focus that can be successfully removed, is rather simplistic.

Conclusion

As illustrated by this data, ictal hypermotor semiology correlated with direct activation of the cingulate cortex. Subsequent seizure propagation in this patient activated an extensive extra-cingulate, rather than intra-cingulate epileptogenic, network. This study highlights the need for further studies exploring the propagation of seizures arising from the cingulate gyrus and the physiological and pathological connectivity patterns within the cingulate gyrus in humans. □

Acknowledgements and disclosures.
RA wishes to acknowledge research support by the American Epilepsy Society and CTSA Grant Number UL1 TR000142 from the National Center for Advancing Translational Science (NCATS), a component of the National Institutes of Health (NIH). RA and NG wish to acknowledge the generous support of the Swebilius trust.
None of the authors have any conflict of interest to disclose.

References

Alkawadri R, Mickey BE, Madden CJ, Van Ness PC. Cingulate gyrus epilepsy: clinical and behavioral aspects, with surgical outcomes. *Arch Neurol* 2011; 68: 381-5.

Alkawadri R, So NK, Van Ness PC, Alexopoulos AV. Cingulate epilepsy: report of 3 electroclinical subtypes with surgical outcomes. *JAMA Neurol* 2013; 70: 995-1002.

Arikuni T, Sako H, Murata A. Ipsilateral connections of the anterior cingulate cortex with the frontal and medial temporal cortices in the macaque monkey. *Neurosci Res* 1994; 21: 19-39.

Bancaud J, Talairach J. Clinical semiology of frontal lobe seizures. *Adv Neurol* 1992; 57: 3-58.

Bancaud J, Talairach J, Geier S, Bonis A, Trottier S, Manrique M. Behavioral manifestations induced by electric stimulation of the anterior cingulate gyrus in man. *Rev Neurol (Paris)* 1976; 132: 705-24.

Brodmann K. *Vergleichende Lokalisationslehre der Grosshirnrinde in ihren Prinzipien dargestellt auf Grund des Zellenbaues*. Leipzig: Johann Ambrosius Barth Verlag, 1909.

David O, Blauwblomme T, Job AS, *et al*. Imaging the seizure onset zone with stereo-electroencephalography. *Brain* 2011; 134: 2898-911.

Devinsky O, Morrell MJ, Vogt BA. Contributions of anterior cingulate cortex to behaviour. *Brain* 1995; 118(1): 279-306.

Garzon E, Lüders HO. *Textbook of epilepsy surgery*. Leipzig: Informa UK Ltd, 2008.

Guedj E, McGonigal A, Vaugier L, Mundler O, Bartolomei F. Metabolic brain PET pattern underlying hyperkinetic seizures. *Epilepsy Res* 2012; 101: 237-45.

Koubeissi MZ, Jouny CC, Blakeley JO, Bergey GK. Analysis of dynamics and propagation of parietal cingulate seizures with secondary mesial temporal involvement. *Epilepsy Behav* 2009; 14: 108-12.

Lee SA, Spencer DD, Spencer SS. Intracranial EEG seizure-onset patterns in neocortical epilepsy. *Epilepsia* 2000; 41: 297-307.

Mazars G. Criteria for identifying cingulate epilepsies. *Epilepsia* 1970; 11: 41-7.

Schiller Y, Cascino GD, Busacker NE, Sharbrough FW. Characterization and comparison of local onset and remote propagated electrographic seizures recorded with intracranial electrodes. *Epilepsia* 1998; 39: 380-8.

Seltzer B, Pandya DN. Posterior cingulate and retrosplenial cortex connections of the caudal superior temporal region in the rhesus monkey. *Exp Brain Res* 2009; 195: 325-34.

Talairach J, Bancaud J, Geier S, *et al*. The cingulate gyrus and human behaviour. *Electroencephalogr Clin Neurophysiol* 1973; 34: 45-52.

Unnwongse K, Wehner T, Foldvary-Schaefer N. Mesial frontal lobe epilepsy. *J Clin Neurophysiol* 2012; 29: 371-8.

Velasco AL, Wilson CL, Babb TL, Engel Jr. J. Functional and anatomic correlates of two frequently observed temporal lobe seizure-onset patterns. *Neural Plast* 2000; 7: 49-63.

Vogt BA, Laureys S. Posterior cingulate, precuneal and retrosplenial cortices: cytology and components of the neural network correlates of consciousness. *Prog Brain Res* 2005; 150: 205-17.

Vogt BA, Finch DM, Olson CR. Functional heterogeneity in cingulate cortex: the anterior executive and posterior evaluative regions. *Cereb Cortex* 1992; 2: 435-43.

Vogt BA, Vogt LJ, Perl DP, Hof PR. Cytology of human caudomedial cingulate, retrosplenial, and caudal parahippocampal cortices. *J Comp Neurol* 2001; 438: 353-76.

Vogt BA, Vogt L, Farber NB, Bush G. Architecture and neurocytology of monkey cingulate gyrus. *J Comp Neurol* 2005; 485: 218-39.

Vogt BA, Vogt L, Laureys S. Cytology and functionally correlated circuits of human posterior cingulate areas. *Neuroimage* 2006; 29: 452-66.

Wendling F, Bartolomei F, Bellanger JJ, Bourien J, Chauvel P. Epileptic fast intracerebral EEG activity: evidence for spatial decorrelation at seizure onset. *Brain* 2003; 126: 1449-59.

Wong CH, Mohamed A, Larcos G, McCredie R, Somerville E, Bleasel A. Brain activation patterns of versive, hypermotor, and bilateral asymmetric tonic seizures. *Epilepsia* 2010; 51: 2131-9.

Yakovlev PI, Locke S. Limbic nuclei of thalamus and connections of limbic cortex. III. Corticocortical connections of the anterior cingulate gyrus, the cingulum, and the subcallosal bundle in monkey. *Arch Neurol* 1961; 5: 364-400.

Zaveri HP, Williams WJ, Sackellares JC, Beydoun A, Duckrow RB, Spencer SS. Measuring the coherence of intracranial electroencephalograms. *Clin Neurophysiol* 1999; 110: 1717-25.